

The room temperature strengthening effect of boron as a function of aluminum concentration in FeAl

I. Baker,^{a*} X. Li,^a H. Xiao,^a R. Carleton^b & E. P. George^b

^a*Thayer School of Engineering, Dartmouth College, Hanover, New Hampshire 03755, USA*

^b*Metals and Ceramics Division, Oak Ridge National Laboratory, Oak Ridge, Tennessee 37831, USA*

(Received 21 January 1997; accepted 20 May 1997)

Measurements of the effects of boron on the yield strength, lattice parameter, vacancy concentration and anti-site atom concentration of FeAl as a function of aluminum concentration have been performed and the results compared with data for similar but undoped FeAl. It has been shown that boron does not affect the degree of order, vacancy concentration or anti-site atom concentration in FeAl. Boron produces an increase in lattice parameter in FeAl but both this increase and the lattice strain per atomic percent boron decrease with increasing aluminum concentration. The effect of boron on the strength of FeAl depends on whether vacancies are present. For FeAl containing few vacancies (≤ 45 at %Al) the strength increase per atomic percent boron increases with increasing aluminum concentration; when vacancies are present (≥ 48 at %Al), boron strengthening shows little change with aluminum concentration, suggesting that the vacancies affect the boron strengthening mechanism. The strength increase per unit increase in lattice parameter depends on the aluminum concentration and is 0.23–0.80 G, where G is the shear modulus. © 1997 Elsevier Science Limited

Key words: A. iron aluminides (based on FeAl), B. mechanical properties at ambient temperatures, C. casting, extrusion, D. defects: constitutional vacancies, mechanical testing.

INTRODUCTION

Boron is a common additive to many intermetallic compounds since it not only increases the strength but in some cases also improves the low temperature ductility, although this can be at the expense of the elevated temperature ductility. There have been a number of measurements of the yield strength of boron-doped FeAl^{1–11} and, in principle, one could use these to determine the strengthening effect of boron by comparing with the strength of unalloyed FeAl.^{12–14} However, it is difficult to assess the boron strengthening effect this way since the alloys studied typically had other elemental additions, fine-grains and/or different heat-treatments. In this paper we examine the effect of boron on the strength and lattice parameter of large-grained, low-temperature annealed FeAl as a function of aluminum concentration and compare

the results with those for unalloyed but otherwise identical FeAl reported previously.¹⁴

EXPERIMENTAL

Ingots of five FeAl alloys (40, 43, 45, 48 and 50 at% Al) containing 0.12 at% B were cast and extruded (canned in mild steel) at 1173 K at a 9:1 area reduction ratio. A few particles, possibly borides, were noted in this material using transmission electron microscopy.¹⁵ However, since they were quite rare, they have negligible effects on the strengths, lattice parameters or boron in solution. To determine the strengthening effect of boron, cylindrical compression specimens (5 mm dia. × 10 mm high) were ground from the extruded rods and annealed at ~1173 K for Fe–40Al, Fe–43Al and Fe–45Al, at ~1473 K for Fe–48Al and Fe–50Al to obtain large grain sizes (~250–300 μm). The use of the large grain sizes was to circumvent the substantial grain

*To whom correspondence should be addressed.

boundary strengthening observed in these materials¹² which might otherwise obfuscate the effects of boron. The annealed rods were slowly cooled at 30 K h⁻¹ and then annealed at 673 K for ~120 h in order to remove the retained vacancies.¹⁶ The specimens were electro-polished in 10% perchloric acid/90% methanol prior to compression testing in air at an initial strain rate of $\sim 1 \times 10^{-4}$ s⁻¹.

For X-ray diffraction studies, powders were filed from each boron-doped alloy; ground, to reduce the particle size; sieved to -400 mesh (< 25 μ m); annealed in argon for 1 h at 1073 K; furnace-cooled; and re-annealed at 673 K for 120 h.

To determine the lattice parameters, Debye-Scherrer X-ray diffraction patterns were obtained from the powders using a Straumanis camera and Ni-filtered Cu K α radiation. The $2\theta = 0^\circ$ and $2\theta = 180^\circ$ positions on the resulting X-ray pattern, corresponding to the incident beam and transmitted beam positions, were defined by averaging measurements of lines corresponding to the same $\{hkl\}$ values on either side of these positions. Line positions could be measured to better than ± 0.03 mm giving an error in lattice parameter measurements of better than $\pm 2 \times 10^{-4}$ Å or approximately one part in 10 000. The best value of the lattice parameter of each alloy, a_0 , was obtained from a linear regression analysis of the measured lattice parameter, a , (for $\theta > 45^\circ$) plotted against the Nelson-Riley function, $N-R = 1/2 [\cos^2 \theta / \sin \theta + \cos^2 \theta / \theta]$,¹⁷ and extrapolated to $N-R = 0$. Similar measurements were performed on five powders of FeAl with the same aluminum concentrations as those noted above but without boron. The processing of these alloys was very similar and has been described elsewhere.¹⁴

To determine whether the vacancy concentrations and anti-site atom concentrations were affected by the presence of boron, X-ray diffractometer traces were also obtained from each of the five boron-doped alloy powders using a Siemens D5000 equipped with a copper tube operated at 40 kV and 30 mA. A Kevex solid state detector was used to count the diffracted Cu K α radiation. Measurements were performed by step scanning 2θ from 28 to 120° in 0.01° steps for typically 10s per step. For each alloy, three separate measurements were made with the powder unloaded and reloaded between measurements and the three results averaged.

The integrated intensity of each diffracted X-ray peak, I_{hkl} , was calculated¹⁷ from

$$I_{hkl} = Kp \left(\frac{1 + \cos^2 \theta}{\sin^2 \theta \cos \theta} \right) e^{-2M} |F|^2 \quad (1)$$

where F is the structure factor, p is the multiplicity factor, $(1 + \cos^2 2\theta / \sin^2 \theta / \cos \theta)$ is the Lorentz-polarization factor, K is a scale factor which is independent of the reflecting planes, e^{-2M} is the temperature factor, and M can be expressed using a single parameter, B , through

$$M = B(\sin \theta / \lambda)^2 \quad (2)$$

where λ is the wavelength of the X-rays. B was obtained through a linear regression analysis,

$$\log[I_{cal}(O)/I_{obs}] = 2B(\sin \theta / \lambda)^2 - \log K \quad (3)$$

where I_{obs} is the observed integrated intensity for a particular peak and

$$I_{cal}(O) = I_{cal}/e^{-2M} = \left[\frac{1 + \cos^2 2\theta}{\sin^2 \theta \cos \theta} \right] p |F|^2 \quad (4)$$

where I_{cal} and $I_{cal}(0)$ are the calculated intensities and $I_{cal} = I/K$ (see eqn (1)) is independent of the scale factor K . Thus, $I_{cal}(0)$ is independent of both the temperature factor and the scale factor. The slope of a plot of $\log[I_{cal}(0)/I_{obs}]$ versus $(\sin \theta / \lambda)^2$ yields B and hence the temperature factor from eqn (2).

The measured integrated intensities can be used to determine the vacancies and anti-site atoms present by comparing with the calculated integrated intensities. (Since boron is a light element, occupies interstitial sites in FeAl and is present at only a very low concentration, it can be neglected from calculations of X-ray intensities.) The calculated integrated intensities can be formulated as follows.¹⁴ The fractional site occupancies of anti-site atoms and vacancies can be written:

$$Y_{Fe/Fe} + Y_{Al/Fe} + Y_{V/Fe} = Y_{Al/Al} + Y_{Fe/Al} + Y_{V/Al} = 1 \quad (5)$$

where $Y_{Fe/Fe}$, $Y_{Al/Fe}$ and $Y_{V/Fe}$ are the fractions of Fe atoms, Al atoms and vacancies that occupy the Fe-sites and $Y_{Al/Al}$, $Y_{Fe/Al}$ and $Y_{V/Al}$ are the fraction of Al atoms, Fe atoms and vacancies that occupy the Al-sites, respectively.

In FeAl, the frequently-occurring defect is the triple-defect,¹⁸ consisting of an Fe atom on the Al-site, and two vacancies on the Fe-site. If we assume that Al atoms do not substitute for the Fe atoms, and for both Fe-rich and stoichiometric compositions there are no vacancies on Al sites, that is, $Y_{V/Al} = Y_{Al/Fe} = 0$, then, eqn (5) can be rewritten as

$$Y_{Fe/Fe} + Y_{V/Fe} = Y_{Al/Al} + Y_{Fe/Al} = 1 \quad (6)$$

The atomic fraction of Fe atoms in the alloy can be expressed as

$$X_{\text{Fe}} = \frac{Y_{\text{Fe/Fe}} + Y_{\text{Fe/Al}}}{Y_{\text{Al/Al}} + Y_{\text{Al/Fe}} + Y_{\text{Fe/Fe}} + Y_{\text{Fe/Al}}} \quad (7)$$

where, as noted above, $Y_{\text{Al/Fe}} = 0$. The atomic fraction of Al atoms, X_{Al} , can be obtained from

$$X_{\text{Al}} = 1 - X_{\text{Fe}} \quad (8)$$

From eqns (7) and (8) one can obtain

$$Y_{\text{Fe/Fe}} = \frac{X_{\text{Fe}}}{X_{\text{Al}}} (1 - Y_{\text{Fe/Al}}) - Y_{\text{Fe/Al}} \quad (9)$$

The structure factor for fundamental reflections in FeAl ($h+k+l=\text{even}$) is given by

$$F_f = (Y_{\text{Fe/Fe}} + Y_{\text{Fe/Al}})f_{\text{Fe}} + (Y_{\text{Al/Fe}} + Y_{\text{Al/Al}})f_{\text{Al}} \quad (10a)$$

and that for superlattice reflections ($h+k+l=\text{odd}$) by

$$F_s = (Y_{\text{Fe/Fe}} - Y_{\text{Fe/Al}})f_{\text{Fe}} - (Y_{\text{Al/Al}} - Y_{\text{Al/Fe}})f_{\text{Al}} \quad (10b)$$

Thus, using eqn (9), the structure factor for fundamental reflections can be rewritten as

$$F_f = \frac{X_{\text{Fe}}}{X_{\text{Al}}} (1 - Y_{\text{Fe/Al}})f_{\text{Fe}} + (1 - Y_{\text{Fe/Al}})f_{\text{Al}} \quad (11a)$$

and that for superlattice reflections ($h+k+l=\text{odd}$) as

$$F_s = \left[\frac{X_{\text{Fe}}}{X_{\text{Al}}} (1 - Y_{\text{Fe/Al}}) - 2Y_{\text{Fe/Al}} \right] f_{\text{Fe}} - (1 - Y_{\text{Fe/Al}})f_{\text{Al}} \quad (11b)$$

The structure factors in eqns (11a) and (11b) are written in terms of only one unknown quantity, $Y_{\text{Fe/Al}}$. Using these structure factors, the calculated integrated intensities for the {100} superlattice and {200} fundamental reflections are obtained from

$$\left\{ \frac{I_{(100)}}{I_{(200)}} \right\}_{(cal.)} = \frac{\left\{ \left(\frac{1+\cos^2 2\theta}{\sin^2 \theta \cos \theta} \right) e^{-2M} |F_s|^2 \right\}_{(100)}}{\left\{ \left(\frac{1+\cos^2 2\theta}{\sin^2 \theta \cos \theta} \right) e^{-2M} |F_f|^2 \right\}_{(200)}} \quad (12)$$

This can be compared to the measured value $I_{(100)}/I_{(200)}$ (meas.) in order to obtain $Y_{\text{Fe/Al}}$.

The measured long range order parameter (S) can be obtained from

$$S_{meas} = \sqrt{\frac{I_{(100)}/I_{(200)}(obs.)}{I_{(100)}/I_{(200)}(cal.)}} \quad (13)$$

where $I_{(100)}/I_{(200)}(cal.)$ in this case is calculated assuming no vacancies are present and that excess Fe atoms substitute on the other (aluminum) sublattice site but that there are no other anti-site atoms than these. The maximum degree of order for stoichiometric and Fe-rich FeAl is given by

$$S_{\text{Al}}^{max} = 2X_{\text{Al}} \quad (14)$$

For the stoichiometric composition, maximum order means that there are no vacancies present and all Fe and Al atoms occupy their own sites. For iron-rich FeAl, maximum order means that no vacancies exist and the excess Fe atoms substitute on the other (aluminum) sublattice site. If $S_{meas} \approx S_{\text{Al}}^{max}$, maximum order is achieved and no constitutional vacancies are present. If $S_{meas} < S_{\text{Al}}^{max}$, $Y_{\text{Fe/Al}}$, can be calculated from eqn (12) as described above. Then, $Y_{\text{Fe/Fe}}$, $Y_{\text{V/Fe}}$, and $Y_{\text{Al/Al}}$ can be obtained from eqns (6) and (9).

RESULTS AND DISCUSSION

The results for boron-doped FeAl alloys are presented along with the results by Xiao and Baker¹⁴ on non-boron-doped FeAl alloys that were processed identically. Figure 1 shows the measured

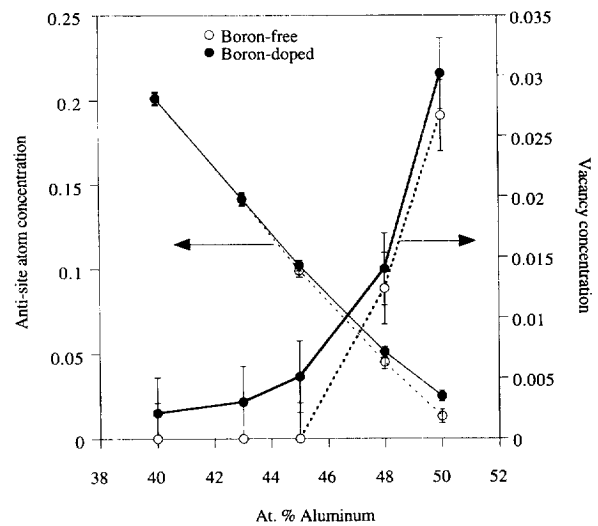


Fig. 1. Concentrations of Fe anti-site atoms on the aluminum sublattice, $Y_{\text{Fe/Al}}$, and vacancies on the iron sublattice, $Y_{\text{V/Fe}}$, as a function of aluminum concentration. The data for unalloyed FeAl are from Ref. 14.

Table 1. Comparison of the measured long range order parameter, S_{meas} , with the calculated maximum possible value, S_{Al}^{max} , for boron-doped FeAl alloys. The \pm indicates the largest deviation of three measurements

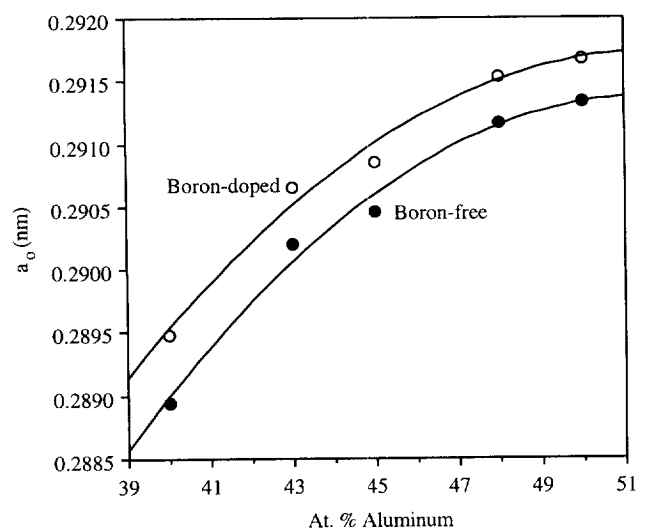
Composition	Fe-40	Fe-43Al	Fe-45Al	Fe-48Al	Fe-50Al
S_{Al}^{max}	0.80	0.86	0.90	0.96	1.00
S_{meas} (B-free)	0.79 ± 0.02	0.85 ± 0.02	0.91 ± 0.01	0.94 ± 0.01	0.94 ± 0.02
S_{meas} B-doped	0.79 ± 0.03	0.85 ± 0.03	0.89 ± 0.03	0.94 ± 0.03	0.96 ± 0.03

concentration of Fe anti-site atoms on the aluminum sub-lattice and vacancies on iron sites as a function of atomic percent aluminum for FeAl with and without boron, determined by the X-ray methods outlined above. It is worth re-iterating that in order to derive eqns (11) from which the data in Fig. 1 are derived, the concentrations of Al anti-site atoms on the iron sub-lattice and vacancies on the aluminum sites were assumed to be zero. There are some X-ray data which indicate that perhaps 6% of the Fe sub-lattice sites are occupied by Al irrespective of the Fe:Al ratio.¹⁹ However, it is worth noting that in that study the vacancy concentrations were assumed to be zero. Thus, the anti-site atom concentrations may be somewhat higher than indicated in Fig. 1. However broadly, within experimental error, the data for unalloyed and boron-doped FeAl are similar, that is, the vacancy concentrations are low from 40 to 45 at% Al but then increase towards the stoichiometric composition, and the anti-site atom concentrations increase approximately linearly with increasing deviation from the stoichiometric composition. The key point is that boron-doping appears to have little effect on the vacancies and anti-site atoms present. It is worth noting that boron, unlike substitutional elements in FeAl, appears to accelerate the rate at which the equilibrium vacancy concentrations are established during the 120 h at 673 K anneal.²⁰ Table 1 is a comparison of the measured long-range order parameter, S_{meas} , with the maximum possible value, S_{Al}^{max} obtained from eqn (14). Again, within experimental error, the values for boron-doped FeAl are the same as those for unalloyed FeAl.¹⁴ The measured values for the alloys containing few vacancies (40–45 at% Al) are very close to the theoretical values, suggesting that sample granularity effects on the X-ray intensities arising from the large particle size²¹ are not significant in the present study.

The compositional dependence of the lattice parameter for both boron-doped FeAl and unalloyed FeAl is shown in Fig. 2. (Each point is the average of three measurements.) Boron leads to an increase in lattice parameter at all compositions.

The boron atoms being smaller than either the iron or aluminum atoms must occupy interstitial sites to cause this lattice expansion. Recent hard-sphere modeling of interstitial sites in B2 compounds²² has indicated that the tetrahedral site is always the largest interstitial site, irrespective of the size of the constituent atoms. Thus, it is likely that the boron occupies the tetrahedral interstitial sites. Figure 3 shows the increase in lattice parameter, Δa , (determined from the data in Fig. 2) per unit increase in boron concentration, Δc , as a function of atomic percent aluminum. It is evident that the lattice expansion due to boron decreases with increasing aluminum concentration, and, hence, with increasing lattice parameter. These data are normalized for the lattice parameter change with aluminum concentration by plotting the data in the form of (%) lattice strain, ϵ , = $100\Delta a/\Delta c \times a_0$, as a function of atomic percent aluminum in Fig. 3. Note that there is a change in the slope of both curves on Fig. 3 above 45 at% Al. This change corresponds to the occurrence of vacancies in the material.

The yield stress is shown as a function of atomic percent aluminum for both unalloyed (from Ref. 14) and boron-doped FeAl in Fig. 4. It is evident that boron produces an increase in yield strength,

**Fig. 2.** The lattice parameter for unalloyed and boron-doped FeAl as a function of atomic percent aluminum. Each point is the average of three measurements.

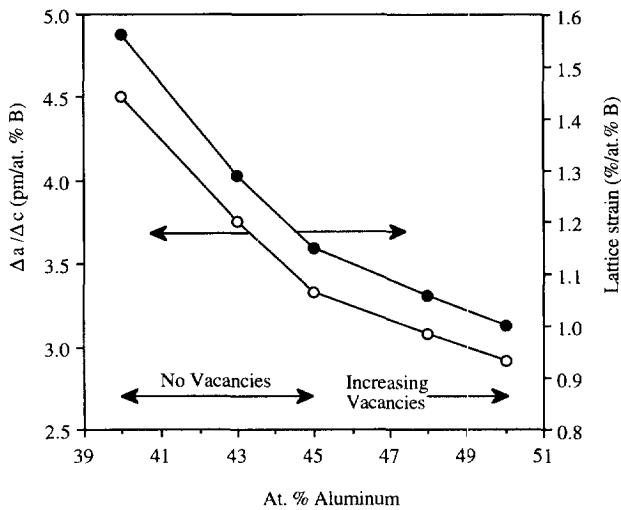


Fig. 3. Change in lattice parameter per unit change in the concentration of boron, $\Delta a_0/\Delta c$, and percentage change in lattice strain, ϵ , as a function of atomic percent aluminum.

$\Delta\sigma_y$, at all aluminum concentrations. The increase in yield strength per atomic percent boron, $\Delta\sigma_y/\Delta c$, is shown as a function of aluminum concentration in Fig. 5. It is worth noting that the yield strength of similarly-processed Fe-45Al doped with only 0.05 at% boron has been measured to be 313 MPa (5), producing a value of $\Delta\sigma_y/\Delta c$, of 860 MPa/at% B, which is very similar to the value of 890 MPa/at% B obtained for the Fe-45Al containing 0.12 at% B measured here. This tends to suggest a linear relationship of yield strength with boron concentration and that the majority of the boron in the alloys was in solution. It is evident in Fig. 5 that in the

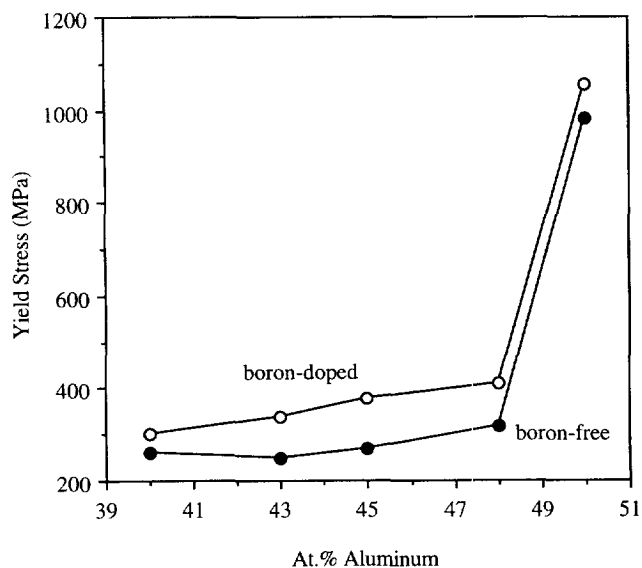


Fig. 4. Yield strength as a function of atomic percent aluminum for large-grained, low temperature annealed boron-doped and unalloyed FeAl. The data for the unalloyed FeAl is from Ref. 14.

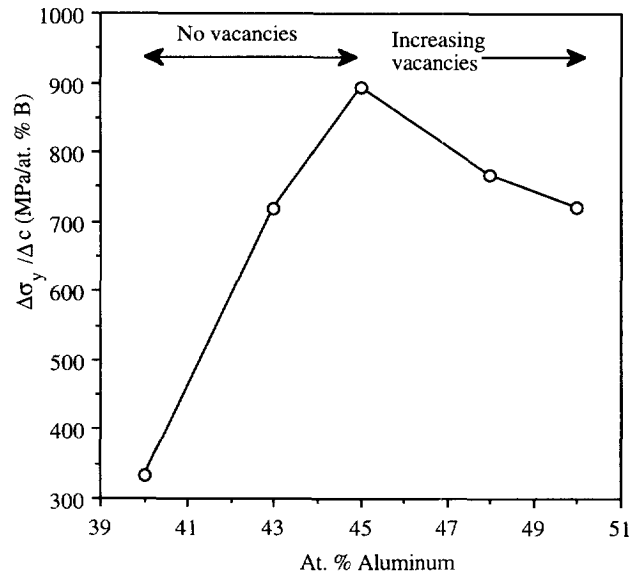


Fig. 5. Increase in yield stress per unit increase in boron concentration $\Delta\sigma_y/\Delta c$ as a function of atomic percent aluminum.

absence of vacancies, i.e. from 40 to 45 at% Al, the strengthening effect of boron increases with increasing aluminum concentration. However, once vacancies are present, i.e. in 48 and 50 at% Al, the strengthening effect decreases. This suggests that the boron atoms are associated with vacancies, i.e. the strain fields due to the lattice expansion from the boron is accommodated by associating with vacancies. The feature is consistent with the decrease in annealing time to reach the equilibrium vacancy concentration in FeAl when boron is present.²⁰

Data from Figs 5 and 6 are combined and replotted in Fig. 6 as $\Delta\sigma_y/(\Delta c \times \epsilon)$, which is also the strength increase per fractional change in lattice parameter, i.e. $\Delta\sigma_y/(\Delta a/a_0)$, as a function of atomic percent aluminum. The data are plotted on the left hand ordinate in terms of their absolute values and on the right hand ordinate normalized with respect to the shear modulus, G . (The shear modulus was calculated using a Poisson's ratio of 1/3 and a Young's modulus of 260 GPa.²³ The latter varies only weakly with composition.)

With the data in the form shown in Fig. 6 it is evident that even though the lattice strain decreases with increasing aluminum (Fig. 3), this is more than offset by the increasing strength with increasing aluminum for alloys containing from 40–45 at% Al. In other words, the data (for 40–45 at% Al) show that the lattice strain alone does not control the strengthening due to boron (otherwise $\Delta\sigma_y/(\Delta c \times \epsilon)$ would be independent of aluminum concentration). Instead, the results indicate that there is chemical dependence to the boron strengthening, i.e. boron strengthening is greater if

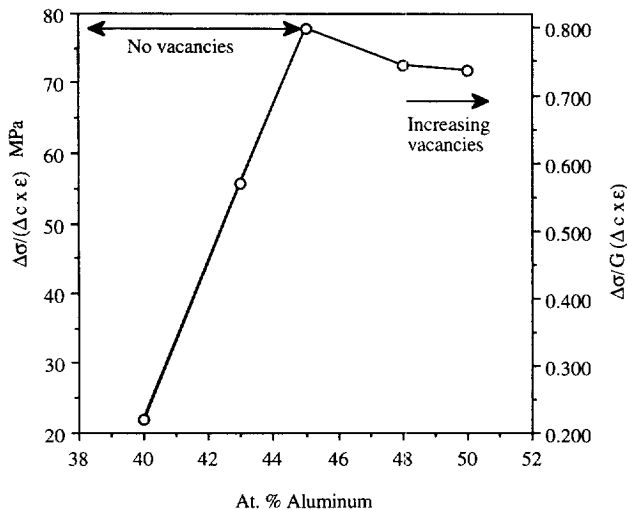


Fig. 6. Strength increase per atomic percent boron per unit strain, $\Delta\sigma_y/(\Delta c \times \epsilon)$ or strength increase per fractional change in lattice parameter as a function of atomic percent aluminum. The left hand ordinate shows the absolute value and the right hand ordinate shows the value normalized with respect to the shear modulus, which itself decreases slightly with increasing aluminum concentration.²³

more aluminum is present. One may speculate that this increased strengthening manifests itself physically through boron's association with the anti-phase boundaries (APBs) between the gliding paired $\frac{a}{2}$ (111) dislocations, (see Refs 24 and 25). Simply on a geometrical basis, interstitial sites are larger there²². Since, the APB energy increases with increasing aluminum concentration in FeAl,²⁶ there may be a tendency for boron atoms to segregate to the APB and to lower its energy with increasing aluminum concentration. This increased segregation to the APB, will cause a greater drag on gliding APB-coupled dislocations and, hence, lead to an increase in strength. This trend would also presumably continue for alloys containing 48 and 50 at% aluminum except that the vacancies present in some way offset this. Perhaps, the strain fields from the boron are ameliorated by the vacancies.

Finally, the strengthening per fractional increase in lattice parameter, $\Delta\sigma_y/(\Delta c \times \epsilon)$, of FeAl due to boron is in the range 0.23 G–0.83 G. This is considerably less than the room temperature strengthening effect of boron in stoichiometric Ni₃Al of 3.76 G.²⁷

CONCLUSIONS

Measurements of the effects of 0.12 at% boron on the yield strength, lattice parameter, vacancy concentration and anti-site atom concentration of

FeAl as a function of aluminum concentration have shown that:

1. Within experimental error, boron does not affect the degree of order, vacancy concentration or anti-site atom concentration in FeAl.
2. Boron produces an increase in lattice parameter but this increase and the related increase in lattice strain per atomic percent boron both decrease with increasing aluminum concentration.
3. The effect of boron on the strength of FeAl depends on whether vacancies are present: for FeAl containing few vacancies (≤ 45 at% Al) the strength increase per atomic percent boron $\Delta\sigma_y/\Delta c$ increases with increasing aluminum concentration; when vacancies are present (≥ 48 at% Al), boron strengthening shows little change with aluminum concentration, suggesting that the vacancies significantly affect the boron strengthening mechanism.
4. The strength increase per unit increase in lattice parameter is 0.22 G–0.80 G depending on the aluminum concentration.

ACKNOWLEDGEMENTS

This work was supported by the U.S. Department of Energy, Office of Basic Energy Sciences, Division of Materials Sciences through contract number DE-FG02-87ER45311 with Dartmouth College, contract DE-AC05-96OR22464 with Lockheed Martin Energy Research Corporation, and through the SHaRE program under contract DE-AC05-76OR00033 with the Oak Ridge Associated Universities. The authors are indebted to Mr Y. Yang and Dr X. Pierron of Dartmouth College and Dr C. J. Sparks of ORNL for useful comments.

REFERENCES

1. Crimp, M. A., Vedula, K. M. and Gaydos, D. J., *Proc. Materials Research Society*, 1987, **81**, 499.
2. Gaydos, D. J., Draper S. L. and Nathal, M. V., *Metall. Trans. A*, 1989, **20A**, 1701.
3. Liu, C. T. and George, E. P., *Scripta Metallurgica et Materialia*, 1990, **24**, 1285.
4. Liu, C. T. and George, E. P., *Proc. MRS*, 1991, **213**, 527.
5. Pike, L. M. and Liu, C. T., *Scripta Metallurgica et Materialia*, 1991, **25**, 2757.
6. Klein, O. and Baker, I., *Scripta Metallurgica et Materialia*, 1992, **27**, 1823.
7. Guo, J. T., Jin, O. Yin, W. M. and Wang, T. M., *Scripta Metallurgica et Materialia*, 1993, **29**, 783.
8. Baker, I., Klein, O., Nelson, C. and George, E. P., *Scripta Metallurgica et Materialia*, 1994, **30**, 863.

9. Klein, O. and Baker, I., *Scripta Metallurgica et Materialia*, 1994, **30**, 627.
10. Carleton, R. L., George, E. P. and Zee, R. H., *Intermetallics*, 1995, **3**, 433.
11. Li, X. and Baker, I., *Scripta Metallurgica et Materialia*, 1996, **34**, 1219.
12. Baker, I., Nagpal, P., Liu, F. and Munroe, P. R., *Acta Metallurgica et Materialia*, 1991, **39**, 1637.
13. Morgund, P., Moururat, P. and Sainfort, G., *Acta Metallurgica*, 1968, **16**, 867.
14. Xiao, H. and Baker, I., *Acta Metallurgica et Materialia*, 1995, **43**, 391.
15. Pierron, X. and Baker, I., *Proc. Materials Research Society*, 1997, **460**, 331.
16. Nagpal, P. and Baker, I., *Metallurgical Transactions*, 1990, **21A**, 2281.
17. Cullity, B. D., *Elements of X-ray Diffraction*, 2nd edn. Addison-Wesley Reading, MA, 1978, p. 139.
18. Chang, Y. A. and Neumann, J. P., *Proc. Solid-State Chem.* ed. W. L. Worrell and G. Rosenbatt. 1982, **14**, 221.
19. Khosla, S., Sparks, C. J., Schneibel, J., Specht, E. D., Jiang, X., Miller, M. K., Zschack, P. and McHargue, C. J., *Proc Cong. on alloy Modelling and Design*, ed. G. M. Stocks and P. E. A. Turchi. TMS Symposium, Pittsburgh, 1993.
20. Gay, A-S., Frackiewicz, A. and Biscondi, M., *Journal de Physique IV*, 1996, **C2**, 153.
21. Sparks, C. J., Kumar, R., Specht, E. D., Zschack, P., Ice, G. E., Shiraishi, T. and Hisatsune, K., *Advances in X-ray Analysis*, eds J. V. Gilfrich, T. C. Huang, R. Jenkins, J. G. McCarthy, P. K. Predicki, R. Ryon and D. K. Smith, Plenum Press, NY, 1992, p. 57.
22. Baker, I., *Journal of Materials Research*, 1993, **8**, 1203.
23. Harmouche, M. R. and Wolfenden, A., *Materials Science and Engineering*, 1986, **84**, 35.
24. Baker, I. and Nagpal, P., in *Structural Intermetallics*, ed. by R. Darolia, J. J. Lewandowski, C. T. Liu, P. L. Martin, D. B. Miracle and M. V. Nathal, The Metallurgical Society, Warrendale, PA., 1993, p. 463.
25. Baker, I., in *Processing, Properties and Applications of Iron Aluminides*, ed. J. H. Schneibel and M. A. Crimp. The Metallurgical Society, Warrendale, PA, 1994, p. 101.
26. Ray, I. L. F., Crawford, R. C. and Cockayne, D. J. H., *Philosophical Magazine*, 1970, **21**, 1027.
27. Baker, I., Huang, B. and Schulson, E. M., *Acta Metallurgica*, 1988, **36**, 493.